Inorg. Chem. **2005**, *44*, 2560–2565

New Oxorhenium(V) Compound for Catalyzed Oxygen Atom Transfer from Picoline *N*-Oxide to Triarylphosphines

Yang Cai, Arkady Ellern, and James H. Espenson*

Ames Laboratory and Department of Chemistry, Iowa State University, Ames, Iowa 50011

Received October 7, 2004

The synthesis and characterization of a new oxorhenium(V) compound is reported; it is [MeReO(edt)(bpym)], **8**, where edt = 1,2-ethanedithiolate and bpym = 2,2′-bipyrimidine. Compound **8** was characterized by NMR spectroscopy and single-crystal X-ray analysis. It exists as a six-coordinate Re(V) compound comparable to the previously known [MeReO(edt)(bpy)] and [MeReO(mtp)(bpy)]. Compound **8** catalyzes the oxygen-atom-transfer reaction PicO + PZ_3 → Pic + Z_3PO, whereas the other two do not. The kinetics of this reaction with catalyst **8** follows the rate law $-d[PicO]/dt = k[\mathbf{8}][PicO]/(1 + c[PZ_3])$. With different phosphines, the rate law has the same k value, 4.17 L mol^{-1} s^{-1}, but different c values. For tritolylphosphine, c = 67.5 L mol^{-1} in benzene at 25 °C. A mechanism has been proposed to account for these findings. The data establish that an open coordination site on rhenium is necessary for oxygen-atom-transfer reactions.

Introduction

Oxygen-atom-transfer (OAT) reactions catalyzed by transition metal complexes have received considerable attention from biological and inorganic chemists.[1,2] Extensive studies have been done with molybdenum and tungsten compounds.[2,3] Certain oxorhenium(V) complexes in Chart 1, such as **1**−**3**, are active catalysts for the following reaction[4,5]

$$PyO + PZ_3 \rightarrow Py + Z_3PO \qquad (1)$$

Until now, the active catalysts have been five-coordinate oxorhenium complexes. In contrast, the six-coordinate rhenium(V) complexes **4**−**7**, Chart 2, do not function as catalysts.[6] It seems that an open coordination site is needed to allow entry of the oxygen atom of the substrate. To test this hypothesis, a potential new catalyst was designed, MeReO(edt)(bpym), **8**, where edt represents 1,2-ethanedithiolate and bpym represents 2,2′-bipyrimidine. The product is a six-coordinate complex with a weakly coordinating bidentate ligand that can be expected to protect the sixth position for subsequent entry of the oxygen donor by making that position available through chelate ring opening. The synthesis and characterization of **8** are reported here, along with studies of the kinetics and mechanism of its catalysis of reaction 1.

Chart 1

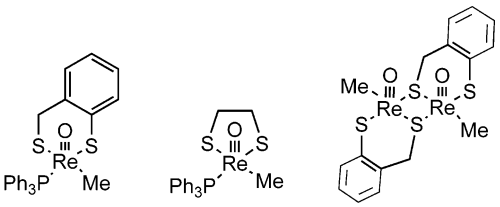

[MeReO(mtp)(PPh$_3$)] **1** [MeReO(edt)(PPh$_3$)] **2** {MeReO(mtp)}$_2$ **3**

Experimental Section

Reagents and Instrumentation. Methyltrioxorhenium(VII) and the dimer {MeReO(edt)}$_2$ were prepared according to literature

* To whom correspondence should be addressed. E-mail: espenson@iastate.edu.

(1) (a) Martiny, L.; Jorgensen, K. A. *J. Chem. Soc., Perkin Trans. 1* **1995**, 699−704. (b) Deubel, D. V.; Sundermeyer, J.; Frenking, G. *Eur. J. Inorg. Chem.* **2001**, 1819−1827.
(2) (a) Holm, R. H. *Chem. Rev.* **1987**, *87*, 1401−1449.
(3) (a) Lorber, C.; Donahue, J. P.; Goddard, C. A.; Nordlander, E.; Holm, R. H. *J. Am. Chem. Soc.* **1998**, *120*, 8102−8112. (b) Donahue, J. P.; Lorber, C.; Nordlander, E.; Holm, R. H. *J. Am. Chem. Soc.* **1998**, *120*, 3259−3260. (c) Donahue, J. P.; Goldsmith, C. R.; Nadiminti, U.; Holm, R. H. *J. Am. Chem. Soc.* **1998**, *120*, 12869−12881. (d) Baird, D. M.; Aburri, C.; Barron, L. S.; Rodriguez, S. A. *Inorg. Chim. Acta* **1995**, *237*, 117−122. (e) Over, D. E.; Critchlow, S. C.; Mayer, J. M. *Inorg. Chem.* **1992**, *31*, 4643−4648. (f) Hall, K. A.; Mayer, J. M. *J. Am. Chem. Soc.* **1992**, *114*, 10402−10411. (g) Shi, Y. L.; Gao, Y. C.; Shi, Q. Z.; Kershner, D. L.; Basolo, F. *Organometallics* **1987**, *6*, 1528−1531. (h) Harlan, E. W.; Berg, J. M.; Holm, R. H. *J. Am. Chem. Soc.* **1986**, *108*, 6992−7000.
(4) (a) Lente, G.; Espenson, J. H. *Inorg. Chem.* **2000**, *39*, 4809−4814. (b) Wang, Y.; Espenson, J. H. *Orga. Lett.* **2000**, *2*, 3525−3526.
(5) Wang, Y.; Espenson, J. H. *Inorg. Chem.* **2002**, *41*, 2266−2274.
(6) Espenson, J. H.; Shan, X.; Lahti, D. W.; Rockey, T. M.; Saha, B.; Ellern, A. *Inorg. Chem.* **2001**, *40*, 6717−6724.

10.1021/ic048598p CCC: $30.25
Published on Web 03/04/2005

Chart 2

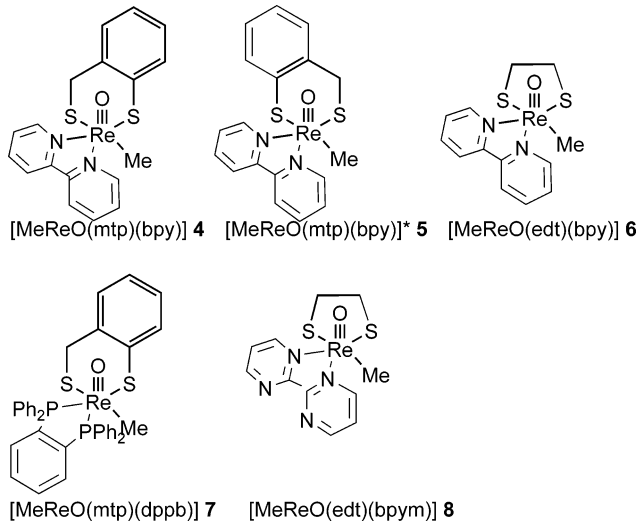

procedures.[7] Other reagents were purchased from commercial sources and used as received. Benzene was the solvent for all studies.

A Bruker DRX-400 MHz spectrometer was used to record ^{1}H and ^{31}P NMR spectra. The ^{1}H chemical shifts were referenced internally using the residual proton resonance of the solvent, C_6D_6, and ^{31}P chemical shifts to 85% H_3PO_4. The elemental analysis of compound **8** was performed by Desert Analytics Laboratory, Tucson, AZ.

Synthesis and Characterization of 8. {MeReO(edt)}$_2$ (30 mg, 0.049 mmol) was dissolved in toluene (10 mL), and 2 equiv of 2,2′-bipyrimidine (bpym) was then added. The color changed from brown to deep red in 1 h. After being stirred for about 6 h, the solution was concentrated to ca. 3 mL by rotary evaporation, and the product was precipitated by addition of hexanes. Compound **8**, [MeReO(edt)(bpym)], was obtained as a dark red solid in 54% yield. ^{1}H NMR (C_6D_6, 25 °C, Figure 1): δ 2.83 (s, 3H, CH_3), 3.07 (m, 1H, CH_2), 3.15 (m, 1H, CH_2), 3.33 (m, 1H, CH_2), 3.79 (m, 1H, CH_2), 5.52 (t, 1H, CH), 5.80 (t, 1H, CH), 7.77 (dd, 2H, CH), 8.25 (d, 1H, CH), 9.09 (d, 1H, CH). Elemental analysis for $C_{11}H_{13}N_4OReS_2$ [found (calcd)]: C, 29.04 (28.31); 1H, 2.88 (2.80); N, 11.79 (11.99); S, 13.15 (13.71).

Crystal Structure of 8. A black prismatic crystal with approximate dimensions 0.23 × 0.15 × 0.1 mm^3 was selected under ambient conditions. The crystal was mounted and centered in the X-ray beam by using a video camera. The crystal evaluation and data collection were performed at 173 K on a Bruker CCD-1000 diffractometer with Mo Kα (λ = 0.71073 Å) radiation and a detector-to-crystal distance of 5.03 cm. The initial cell constants were obtained from three series of ω scans at different starting angles. Each series consisted of 30 frames collected at intervals of 0.3° in a 10° range about ω with the exposure time of 10 s per frame. A total of 189 reflections were obtained. The reflections were successfully indexed by an automated indexing routine built into the SMART program. The final cell constants were calculated from a set of 1428 strong reflections from the actual data collection. The data were collected using the full-sphere routine. A total of 4208 data were harvested by collecting four sets of frames with 0.3° scans in ω with an exposure time of 10 s per frame. This dataset was corrected for Lorenz and polarization effects. The absorption correction was based on fitting a function to the empirical transmission surface as sampled by multiple equivalent measurements[8] using SADABS software.[9]

Table 1. Crystal Data and Structure Refinement for [MeReO(edt)(bpym)] **8**

chemical formula	$C_{11}H_{13}N_4OReS_2$
formula weight	467.57
crystal system	monoclinic
space group	$P2(1)/c$
unit cell dimensions	a = 13.547(3) Å, α = 90°
	b = 8.056(2) Å, β = 103.227(4)°
	c = 12.984(3) Å, γ = 90°
volume	1379.4(6) Å^3
Z	4
density (calculated)	2.251 Mg/m^3
absorption coefficient	9.108 mm^{-1}
GOF on F^2	1.042
R1, wR2 [$I > 2\sigma(I)$]	0.0156, 0.0392
R1, wR2 (all data)	0.0163, 0.0395

The systematic absences in the diffraction data were consistent with the space group $P21/c$, which yielded chemically reasonable and computationally stable results of refinement. The position of the heavy atom was found by the Patterson method. The remaining atoms were located in an alternating series of least-squares cycles and difference Fourier maps. All non-hydrogen atoms were refined in a full-matrix anisotropic approximation. All hydrogen atoms were found objectively and were allowed to ride on the neighboring atoms with relative isotropic displacement coefficients. Final least-squares refinement of 172 parameters against 1988 independent reflections converged to R (based on F^2 for $I \geq 2\sigma$) and wR (based on F^2 for $I \geq 2\sigma$) values of 0.016 and 0.039, respectively. The basic details of the structural solution are given in Table 1, and further parameters are reported in the Supporting Information.

Kinetics. The reactions of 4-picoline *N*-oxide (PicO) and triarylphosphines (PZ^3) were monitored by the integration of the methyl peaks of PicO and 4-picoline (Pic). The phosphine was added in greater than 10-fold excess, allowing the concentration−time data to be fitted by pseudo-first-order kinetics eq 2

$$[\mathrm{PicO}]_t = [\mathrm{PicO}]_0 e^{-k_{obs}t} \qquad (2)$$

Results and Discussion

Structure of 8. Figure 2 shows the molecular structure of compound **8**. The rhenium atom is six-coordinate, located in the center of a distorted octahedron. Table 2 lists selected bond distances and angles. The Re−O bond length is 169.2(3) pm, which is quite similar to those found in most well-characterized Re(V) oxo compounds.[10] As reported in the literature, the distances for idealized Re^V≡O and Re^V═O bonds were estimated to be approximately 160 and 176 pm, respectively.[10,11] The Re−N(1) bond distance of 226.4 pm for the N that lies trans to the oxo group is longer than that of Re−N(3), 218.6 pm, for N trans to a sulfur atom. This is due to the trans influence of the terminal oxo group

(7) (a) Herrmann, W. A.; Kratzer, R. M.; Fischer, R. W. *Angew. Chem., Int. Ed. Engl.* **1997**, *36*, 2652−2654. (b) Espenson, J. H.; Shan, X.; Wang, Y.; Huang, R.; Lahti, D. W.; Dixon, J.; Lente, G.; Ellern, A.; Guzei, I. A. *Inorg. Chem.* **2002**, *41*, 2583−2591.

(8) Blessing, R. H. *Acta Crystallogr.* **1995**, *A51*, 33−38.

(9) All software and sources of the scattering factors are contained in the SHELXTL (version 5.1) program library (Sheldrick, G. Bruker Analytical X-ray Instruments Inc.: Madison, WI, 1997).

(10) (a) Banerjee, S.; Bhattacharyya, S.; Dirghangi, B. K.; Menon, M.; Chakravorty, A. *Inorg. Chem.* **2000**, *39*, 6−13. (b) Edwards, C. F.; Griffith, W. P.; White, A. J. P.; Williams, D. J. *J. Chem. Soc., Dalton Trans.* **1992**, 957−962. (c) Mayer, J. M. *Inorg. Chem.* **1988**, *27*, 3899−3903.

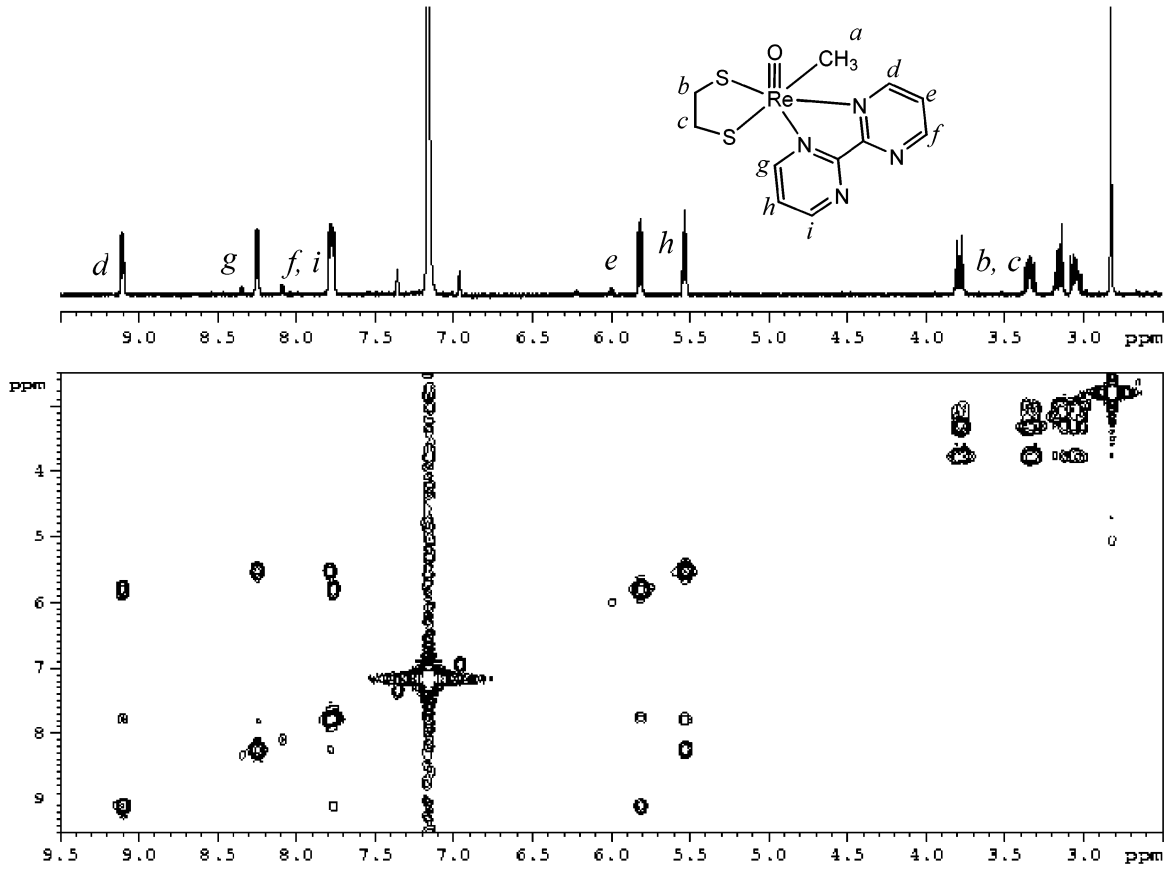

Figure 1. ^{1}H and COSY NMR spectra of compound **8** in C_6D_6 at 25 °C. δ (ppm) 2.83 (s, 3H CH_3), 3.07 (m, 1H, CH_2), 3.15 (m, 1H, CH_2), 3.33 (m, 1H, CH_2), 3.79 (m, 1H, CH_2), 5.52 (t, 1H, CH), 5.80 (t, 1H, CH), 7.77 (dd, 2H, CH), 8.25 (d, 1H, CH), 9.09 (d, 1H, CH).

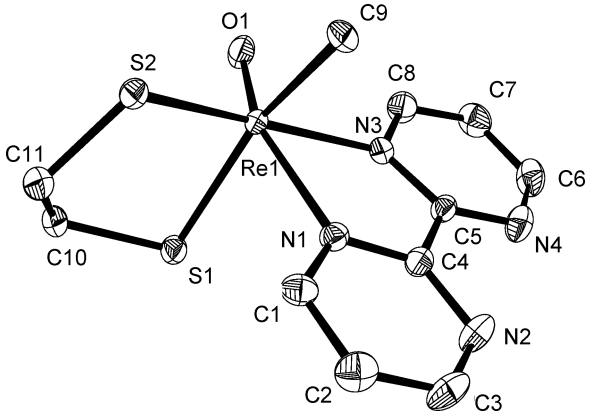

Figure 2. Molecular structure of [MeReO(edt)(bpym)], **8**, with ellipsoids drawn at the 50% probability level.

on rhenium. Further details of the structural parameters are given in Tables S-3−S-6.

Kinetics: An Induction Period. The first system studied was the reaction between 4-picoline *N*-oxide (PicO) and tri-*p*-tolylphosphine ($PTol_3$) in benzene.

As reported previously, no reaction occurred over 10 h in the absence of the catalyst. When 4.17 mM PicO and 50.0 mM $PTol_3$ were mixed, followed by addition of 0.56 mM compound **8**, the reaction went to completion in 3 h as monitored by ^{1}H NMR spectroscopy. A plot of the PicO concentration against time is shown in Figure 3. As one can see, there is an induction period at the beginning of the reaction. When, however, the mixing sequence was changed, different kinetics was found. Mixing either PicO and **8** first and adding $PTol_3$, or mixing $PTol_3$ with **8** and then PicO, gave data without an induction period; the data followed first-order kinetics throughout. The kinetic traces are also presented in Figure 3. The values of the pseudo-first-order rate constant k_{obs} were different in the two cases. The k_{obs} value is 5.4×10^{-4} s^{-1} with $PTol_3$ as the last reagent and 4.3×10^{-4} s^{-1} when PicO was added last. The reason for this difference will be discussed.

Table 2. Selected Bond Lengths (pm) and Angles (deg) in **8**

Re(1)−O(1)	169.2(3)	Re(1)−N(1)	226.4(3)
Re(1)−C(9)	217.5(4)	Re(1)−S(2)	227.33(11)
Re(1)−N(3)	218.6(3)	Re(1)−S(1)	236.75(11)
N(1)−Re(1)−S(2)	96.90(8)	O(1)−Re(1)−N(1)	155.90(11)
O(1)−Re(1)−S(1)	105.09(10)	C(9)−Re(1)−N(1)	77.62(13)
C(9)−Re(1)−S(1)	152.17(11)	N(3)−Re(1)−N(1)	70.78(11)
O(1)−Re(1)−C(9)	102.48(14)	O(1)−Re(1)−S(2)	107.08(9)
O(1)−Re(1)−N(3)	85.16(11)	C(9)−Re(1)−S(2)	83.12(11)
C(9)−Re(1)−N(3)	85.13(13)	N(3)−Re(1)−S(2)	164.59(8)

Determination of the Rate Law. Time-course kinetic analysis was used to determine the dependence of the rate on the concentration of the participating species. The experiments were done under conditions where triarylphos-

(11) (a) Berning, D. E.; Katti, K. V.; Barbour, L. J.; Volkert, W. A. *Inorg. Chem.* **1998**, *37*, 334−339. (b) Smith, C. J.; Katti, K. V.; Volkert, W. A.; Barbour, L. J. *Inorg. Chem.* **1997**, *36*, 3928−3935. (c) Wang, Y. P.; Che, C. M.; Wang, K. Y.; Peng, S. M. *Inorg. Chem.* **1993**, *32*, 5827−5832.

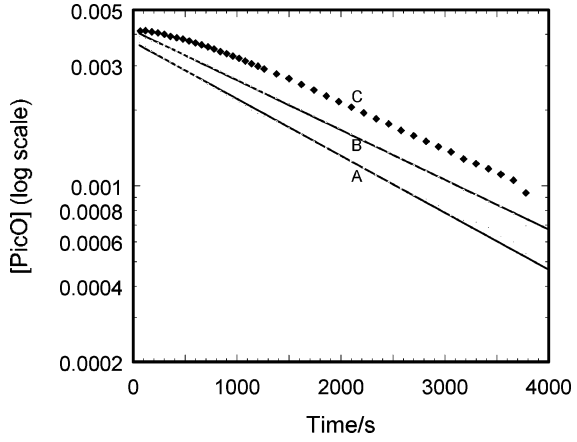

Figure 3. Reactions between picoline *N*-oxide and tritolylphosphine with catalyst **8**. Conditions: 4.17 mM PicO, 50.0 mM $PTol_3$ and 0.56 mM **8** in benzene at 25 °C. (A) $PTol_3$ added last, (B) PicO added last, (C) **8** added last. Note that C shows an induction period, and A has a slightly higher rate constant than B.

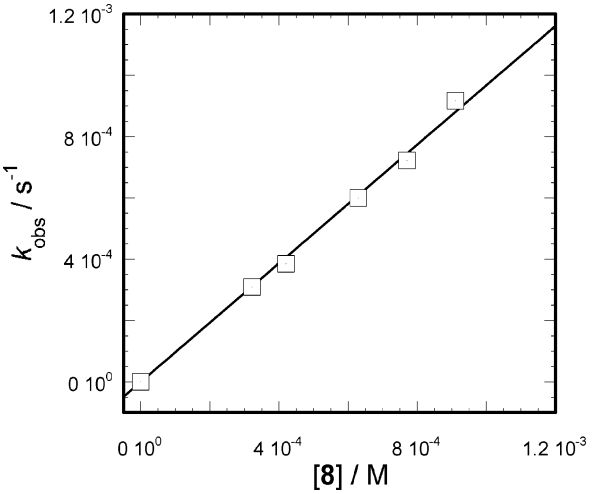

Figure 4. Plot of the pseudo-first-order rate constants vs the concentration of catalyst **8**.

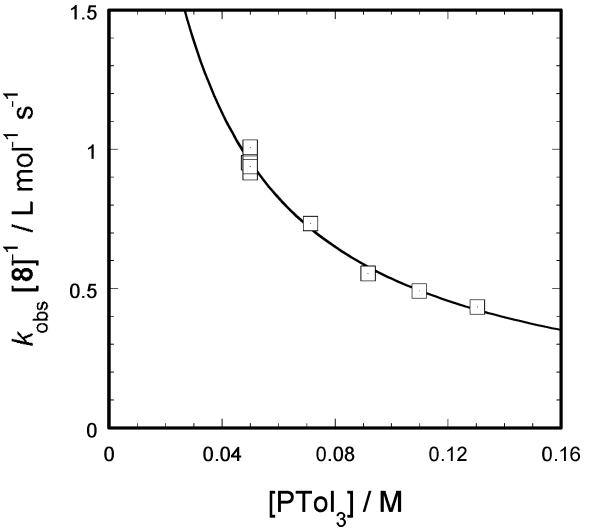

Figure 5. Variation of k_{obs}/[**8**] with the concentration of $PTol_3$ describes a hyperbole.

phine was present in >10-fold excess over picoline *N*-oxide; it was the last reagent added. Generally, the experiments were performed with added 4-picoline and bipyrimidine to avoid any effect from product or complete dissociation of the chelate ligand. In each run, the kinetic data conformed to first-order kinetics, yielding the rate constant k_{obs}. The kinetic data are summarized in Table S-1, which lists the concentrations used in each set of measurements. Figure 4 presents the plot of k_{obs} vs concentration of **8**, establishing that the rate of reaction shows a first-order dependence on catalyst concentration. As for tritolylphosphine, the values of k_{obs}/[**8**] show a nonlinear dependence on the concentration of $PTol_3$, as depicted in Figure 5. The relation is adequately described by eq 3

$$\frac{k_{obs}}{[\mathbf{8}]} = \frac{m_1}{1 + m_2[PTol_3]} \tag{3}$$

These data allow the rate expression for the disappearance of 4-picoline *N*-oxide to be

$$-\frac{d[PicO]}{dt} = \frac{k[\mathbf{8}][PicO]}{1 + c[PTol_3]} \tag{4}$$

where

$$k_{obs} = \frac{k[\mathbf{8}]}{1 + c[PTol_3]} \tag{5}$$

Para-Substituted Phosphines. Kinetic studies for different $P(4\text{-}XC_6H_4)_3$ reagents were carried out with PicO and catalyst **8**, to which eq 5 still applies. The values of k_{obs} for each reaction were obtained by the same method previously described. The resulting pseudo-first-order rate constants for the reactions under investigation are summarized in Table S-2.

It is useful to consider the same set of data from a graphical point of view, to display the effect of phosphine for each term. For that purpose, the expression for k_{obs} in eq 5 can be rearranged to the following form

$$\frac{[\mathbf{8}]}{k_{obs}} = \frac{1}{k} + \frac{c}{k}[PAr_3] \tag{6}$$

On the basis of this relation, the value of [**8**]/k_{obs} should vary linearly with the concentration of triarylphosphine. Such plots for all of para-substituted phosphine complexes investigated are shown in Figure 6. As one can see, they have a common intercept, k^{-1}, but have slopes that differ from one phosphine to another. Table 3 lists the values of k and c for these phosphines. The fastest reactions are those with the most-electron-withdrawing substituent, X = Cl, and vice versa. Further analysis will be presented later.

Reaction Scheme and Chemical Mechanism. On the basis of the kinetic data and the rate law, a possible reaction mechanism is proposed in Scheme 1. According to this scheme, there is an equilibrium between **8** and the half-open chelate species **B**. From crystal data, we know that the Re−N bond trans to the oxo group is weaker; thus it is reasonable

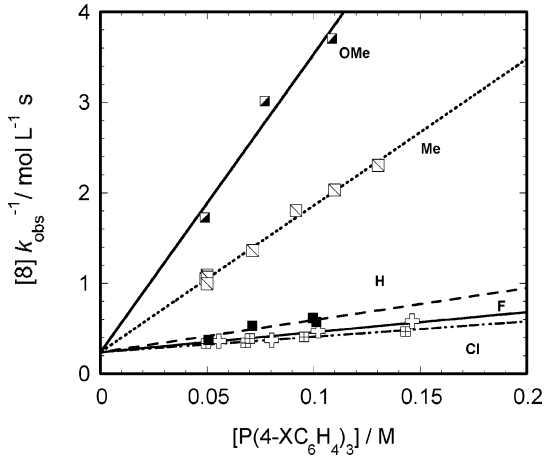

Figure 6. Plot of [**8**]/k_{obs} against concentration of P(4-XC$_6$H$_4$)$_3$ for the reaction between P(4-XC$_6$H$_4$)$_3$ and 4-picoline *N*-oxide catalyzed by **8** at 25 °C in benzene.

Table 3. Values of *k* and *c* in Eq 6 for the Reaction between 4-Picoline *N*-Oxide and P(4-XC$_6$H$_4$)$_3$ Catalyzed by **8** at 25 °C in Benzene

P(4-XC$_6$H$_4$)$_3$	*k*/L mol^{-1} s^{-1}	*c*/L mol^{-1}
X = Cl	4.17	7.04
X = F	4.17	9.17
X = H	4.17	14.8
X = Me	4.17	67.5
X = OMe	4.17	137.2

to postulate that there is a chelate-ring-opening step during the process to start the reaction. Because this step is to some extent thermodynamically unfavorable, only a small amount of **B** would exist in solution. After that, the rhenium species offers a vacant axial position for ligands, such as picoline *N*-oxide or phosphine, to attack and produce six-coordinate rhenium complexes. This ring-opening step also accounts for the induction period observed when picoline oxide and phosphine are mixed first and catalyst added last, because those species need time to reach equilibrium. However, when picoline oxide was first mixed with the catalyst, or phosphine and catalyst were mixed first, no induction period was observed. This phenomenon can be attributed to ligand substitution, which would help to dissociate the sixth ligand and start the catalytic cycle. Compared to the five-coordinate rhenium(V) monodentate phosphine catalysts **1**−**3**, compound **8** is less active by 1−2 orders of magnitude. In addition, as for the previously reported cases, rhenium(V) compounds with strongly coordinating chelates are completely inactive for OAT reactions, which includes 2,2′-bipyridine compounds **4** and **6** and rhenium(V) compound **7** with 1,2-bis(diphenylphosphino)benzene. Clearly, it is important to have an open site at rhenium for catalysis of OAT reactions. For compounds **4**−**7**, the chelate effect is so strong that it is difficult to open a coordination position for the substrate. The difference in Lewis basicity between bipyrimidine and bipyridine is also manifested in the large difference in Brønsted basicities. The pK_a value of LLH$^+$ for bipyrimidine is 0.6, whereas that for bipyridine is 4.4.[12]

Once the half-opened chelate species **B** is produced in the solution, both picoline *N*-oxide and phosphine ligands could coordinate with the rhenium center to make six-coordinate rhenium compounds. If **B** adds picoline *N*-oxide, the catalytic intermediate **C** is formed, and the rate-controlling step then occurs to release picoline and produce a dioxorhenium(VII) intermediate **D**. Finally, **D** transfers an oxygen atom to phosphine in a much more rapid step that gives phosphine oxide, regenerates catalytic intermediate **C**, and continues the catalytic cycle. Therefore, the reaction shows a first-order dependence on picoline *N*-oxide. However, if phosphine coordinates with rhenium, the dead-end species **F** will be formed, which accounts for the inverse dependence on phosphine. In addition, with different interactions of picoline oxides or phosphines to rhenium species, two different rate constants (5.4×10^{-4} vs 4.3×10^{-4} s^{-1}) were found when different addition sequences were used because of the different concentrations of active species in the solution. Adding either picoline oxide or phosphine could push the rhenium species **8** to open the chelate and start the catalytic reaction, but they would do so to different degrees. Although mixing phosphine and **8** first helps produce the active species **B** in the solution, it will also deactivate the catalyst by coordinating phosphine to the rhenium center in **F**. However, this would not happen if picoline oxide were added first. Therefore, the rate constant when phosphine and **8** react first is smaller than that when picoline oxide and **8** are mixed first.

With the catalyst [MeReO(mtp)(PPh$_3$)], the reaction exhibits a second-order dependence on the picoline *N*-oxide concentration,[5] because in that system, the catalytic intermediate needs a second PicO to provide the necessary nucleophilic assistance, as illustrated in Scheme 2.[5,13] In the

Scheme 1. Reaction Mechanism Suggested for OAT between PicO and PPh$_3$ Catalyzed by **8**

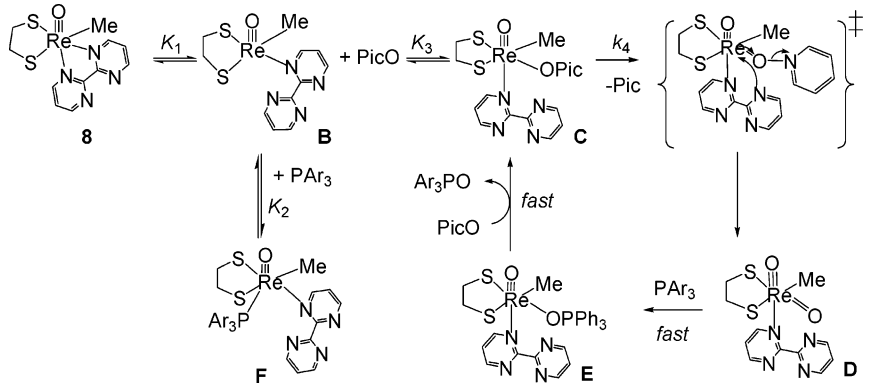

Scheme 2. Nucleophilic Assistance with [MeReO(mtp)(PPh_3)]

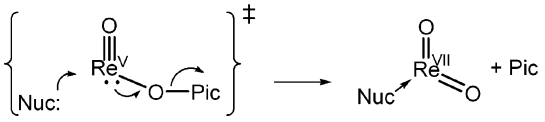

case at hand, however, the chelate ligand bipyrimidine itself plays the role of a nucleophile because it has a free N atom. Note the transition state depicted in Scheme 1.

On the basis of this scheme, a rate expression can be derived by using equilibrium constants

$$\nu = \frac{K_1K_3k_4[\mathrm{PicO}][\mathrm{Re}]_\mathrm{T}}{1 + K_1 + K_1K_3[\mathrm{PicO}] + K_1K_2[\mathrm{PAr_3}]} \qquad (7)$$

As mentioned before, the ring-opening step for **8** is thermodynamically unfavorable, so it is reasonable to assume that K_1 is much less than 1. In addition, large excesses of phosphines over 4-picoline *N*-oxides were used for all experiments examined, and $K_2 \gg K_3$ because of the stronger coordination ability of triarylphosphine than picoline oxide. Therefore, K_1K_3[PicO] should be much smaller than K_1K_2-[PAr_3], and it can be dropped from the denominator in the rate law. Under these assumptions, the rate law is simplified to eq 8, which is exactly the form obtained from the kinetic data

$$\nu = \frac{K_1K_3k_4[\mathrm{PicO}][\mathrm{Re}]_T}{1 + K_1K_2[\mathrm{PAr_3}]} = \frac{k[\mathrm{PicO}][\mathbf{8}]}{1 + c[\mathrm{PAr_3}]} \qquad (8)$$

and with excess phosphine, this becomes

$$k_\mathrm{obs} = \frac{K_1K_3k_4[\mathbf{8}]}{1 + K_1K_2[\mathrm{PAr_3}]} \qquad (9)$$

where $k = K_1K_3k_4$ and $c = K_1K_2$.

Reactivity Trends and Hammett Analysis. The phosphine substrate inhibits oxygen transfer from picoline *N*-oxide to phosphine catalyzed by **8**. This phenomenon can be explained by the equilibrium represented by K_2 in the scheme where phosphine takes up the sixth position to make the six-coordinate rhenium species **F** and thus make a dead end of the catalytic cycle. From Tables S-1 and S-2 in the Supporting Information, it can be seen that the rate increases with an electron-withdrawing group at the para position of the phenyl rings in triarylphosphine. The reason is that triarylphosphine, which has an electron-donating group at the para position, has a better coordination ability. It coordinates to the rhenium center and decelerates the reaction. According to the rate law, *c* in eq 9 represents the combination of equilibrium constants K_1K_2, which refers the interaction between phosphine and **8**. To illustrate this effect, a plot of log(K_1K_2) versus the Hammett substituent constant 3σ is shown in Figure 7, yielding $\rho = -0.93$. The negative ρ value suggests the phosphine coordination ability: the strongest Lewis base gives the greatest equilibrium constant to coordinate with the Re species.

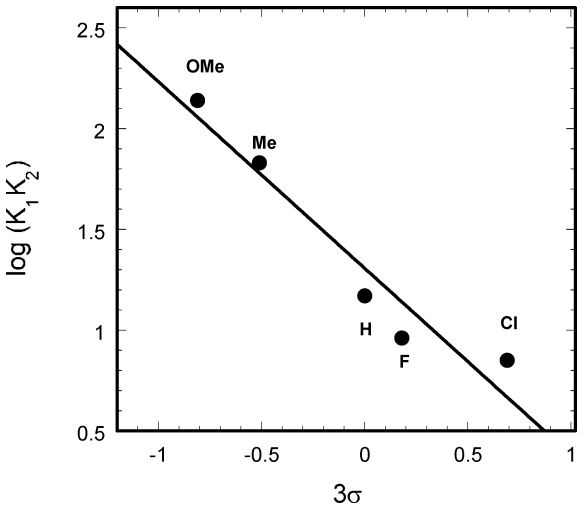

Figure 7. Analysis of the substituent effects in terms of log(K_1K_2) vs the Hammett substituent constant 3σ for the given group X in P(4-XC_6H_4)$_3$.

Acknowledgment. This research was supported by the U.S. Department of Energy, Office of Basic Energy Sciences, Division of Chemical Sciences, under Contract W-7405-Eng-82 with Iowa State University of Science and Technology.

Supporting Information Available: Tables of rate constants, atomic coordinates, bond lengths and angles, anisotropic displacement parameters, and crystal data and refinement details. This material is available free of charge via the Internet at http://pubs.acs.org.

IC048598P

(12) Martell, A. E.; Smith, R. M. *Critical Stability Constants, Vol. 3: Other Organic Ligands*; Plenum Press: New York, 1974. (b) Bly, D. D.; Mellon, M. G. *Anal. Chem.* **1963**, *35*, 1386−1392.
(13) Vasbinder, M. J.; Espenson, J. H. *Organometallics* **2004**, *23*, 3355−3358.